Lattice simulations of the QCD chiral transition at $\mu_B > 0$

Sz. Borsányi [a], **Z. Fodor** [a,b,c,d,e], **M. Giordano** [c], **S. Katz** [c], **D. Nográdi** [c], **A. Pásztor** [c], **C. H. Wong** [a]

[a] Wuppertal University, [b] Penn State University, [c] Eötvös Loránd University, [d] Jülich Supercomputing Centre, [e] UCSD

1. QCD at finite baryochemical potential μ_B

Despite decades of effort, the determination of the phase diagram of strongly interacting matter remains an unsolved problem. From the theoretical side, due to the strongly coupled nature of the theory, a fully non-perturbative, first principles approach - such as lattice QCD - is mandatory. While lattice QCD has revealed much about the case of zero baryochemical potential $\mu_B = 0$ - e.g. that the QCD transition in the early universe was not a true phase transition, but a crossover [1] - the properties of QCD matter at non-zero baryochemical potential remain largely unknown. It is conjectured that the crossover line eventually turns into a line of first order transitions at a critical endpoint. Confirmation of this picture has not yet been achieved, neither by first principle calculations nor by experiment, despite this confimation being a major goal of heavy ion physics. Currently available lattice QCD results at finite density are based on analytic continuation from zero [2] or purely imaginary [3] baryochemical potential. Due to the ill-posed nature of analytic continuation, such methods have severe limitations. Here we use more direct reweighting methods to study thermodynamics at $\mu_B > 0$. This poster is based on Ref. [4].

2. Phase and sign reweighting

Given a target theory, with field variables U, path integral weights $w_t(U)$, and partition function $Z_t = \int \mathcal{D}U\ w_t(U)$, using simulations in a theory with real and positive path integral weights $w_s(U)$ and partition function $Z_s = \int \mathcal{D}U\ w_s(U)$, via reweighting:

$$\langle \mathcal{O} \rangle_t = \left\langle \frac{w_t}{w_s} \mathcal{O} \right\rangle_s \left\langle \frac{w_t}{w_s} \right\rangle_s^{-1}, \quad \langle \mathcal{O} \rangle_x = \frac{1}{Z_x} \int \mathcal{D}U\ w_x(U) \mathcal{O}(U)\,, \tag{1}$$

where x may stand for t (target theory) or s (simulated theory). When the target theory is lattice QCD at non-zero chemical potential μ, the target weights are given by

$$w_t(U) = \det M(U,\mu) e^{-S_g(U)}, \tag{2}$$

where S_g is the gauge action, $\det M$ denotes the fermionic determinant, including all quark types with their respective mass terms, as well as rooting in the case of staggered fermions, and the integral is over the gauge fields U. The weights w_t have fluctuating phases: this is the infamous sign problem of lattice QCD. In addition to this problem, generic reweighting methods also suffer from an overlap problem: the probability distribution of the reweighting factor w_t/w_s has generally a long tail, which cannot be sampled efficiently in standard Monte Carlo simulations. It is actually the overlap problem, rather than the sign problem, that constitutes the immediate bottleneck in QCD when one tries to extend reweighting results to finer lattices [5]. This overlap problem in the weights w_t/w_s is not present if they take values in a compact space. The most well-known of these approaches is phase reweighting [6], where the simulated theory - the so called phase quenched theory - has path integral weights:

$$w_s = w_{PQ} = |\det M_{ud}(\mu)^{\frac{1}{2}}| \det M_s(0)^{\frac{1}{4}} e^{-S_g}. \tag{3}$$

In this case the reweighting factors are pure phases: $(w_t/w_s)_{PQ} = e^{i\theta}$, where $\theta = \mathrm{Arg} \det M$. We will contrast this approach with sign reweighting, where the simulated - sign quenched - ensemble has weights:

$$w_s = w_{SQ} = |\,\mathrm{Re} \det M_{ud}(\mu)^{\frac{1}{2}}| \det M_s(0)^{\frac{1}{4}} e^{-S_g}. \tag{4}$$

In this case the reweighting factor are signs: $(w_t/w_s)_{SQ} = \varepsilon \equiv \mathrm{sign} \cos\theta = \pm 1$, provided that the target theory is the one with $w_t = \mathrm{Re} \det M e^{-S_g}$. The replacement $w_t \to \mathrm{Re}\, w_t$ is not permitted for arbitrary expectation values, but it is allowed for i) observables satisfying either $\mathcal{O}(U^*) = \mathcal{O}(U)$ or ii) observables obtained as derivatives of the partition function with respect to real parameters, such as the chemical potential or the quark mass. Fortunately, these are exactly the observables on needs for bulk thermodynamics.

A key step in addressing the feasibility of our approach is estimating the severity of the sign problem. In the phase quenched (PQ) ensemble the severity of the sign problem is measured by the average phase factor $\langle e^{i\theta} \rangle^{\mathrm{PQ}}_{T,\mu}$, while in the sign quenched (SQ) ensemble it is measured by $\langle \varepsilon \rangle^{\mathrm{SQ}}_{T,\mu}$ The probability distribution of the phases $\theta = \arg \det M$ in the phase quenched theory, $P_{\mathrm{PQ}}(\theta)$, controls the strength of the sign problem in both ensembles. A simple estimate can then be obtained with a wrapped Gaussian approximation of $P_{\mathrm{PQ}}(\theta)$, with the chemical potential dependence of the width given by a leading order Taylor expansion in μ_B. In this model the severity of the sign problem can be calculated analytically [4]. We compare the results from this model to the simulated severity of the sign problem in both ensembles in Fig. 1. The model matches the actual simulation results well, it is therefore straightforward to estimate the required statistics for a given volume and the chemical potential a priori.

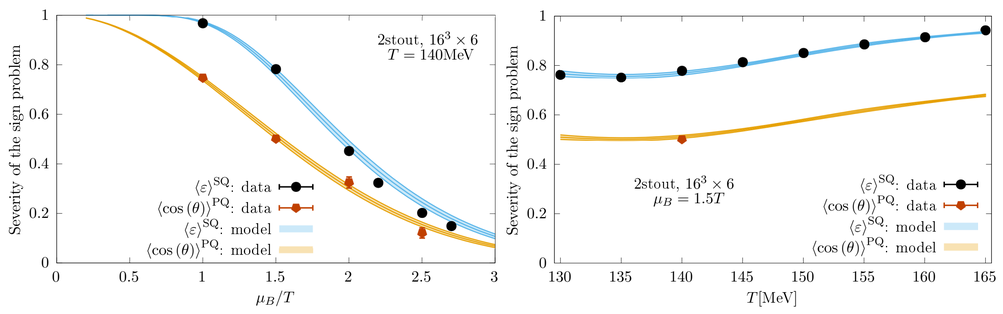

Figure 1: *The strength of the sign problem as a function of μ_B/T at $T = 140$ MeV (left) and as a function of T at $\mu_B/T = 1.5$ (right). A value close to 1 shows a mild, while a value close to 0 indicates a severe sign problem. Data for sign reweighting (black) and phase reweighting (orange) are from direct simulations. Predictions of the Gaussian model are also shown.*

3. Simulation setup

We simulated the sign and phase quenched ensembles for 2+1 flavors of rooted staggered fermions, with a tree-level Symanzik improved gauge action, and two steps of stout smearing with $\rho = 0.15$ on the gauge links fed into the fermion determinant. We use physical quark masses. The scale is set with the kaon decay constant. We studied $16^3 \times 6$ lattices at various temperatures T and light-quark chemical potential $\mu_u = \mu_d = \mu_l = \mu = \mu_B/3$ with a zero strange quark chemical potential $\mu_s = 0$, corresponding to a strangeness chemical potential $\mu_S = \mu_B/3$. We performed a scan in μ_B at fixed $T = 140\,\mathrm{MeV}$, and a scan in temperature at fixed $\mu_B/T = 1.5$. Simulations were performed by modifying the RHMC algorithm at $\mu_B = 0$ by including an extra accept/reject step that takes into account the factor $|\mathrm{Re} \det M(\mu)|/\det M(0)$ or $|\det M(\mu)|/\det M(0)$.

4. Observables and numerical results

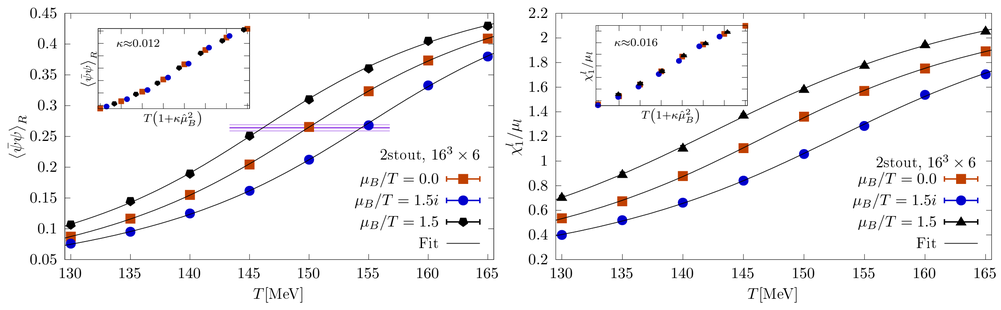

Figure 2: *The renormalized chiral condensate (left) and the light quark number-to-light quark chemical potential ratio (right) as a function of temperature at $\mu_B/T = 1.5$. In the insets, collapse plots are shown in the variable $T \cdot (1 + \kappa \left(\frac{\mu_B}{T}\right)^2)$, with $\kappa \approx 0.012$ for the chiral condensate and $\kappa \approx 0.016$ for the quark number. In the left panel the value of the condensate at the crossover temperature at $\mu_B = 0$ is also shown (by a purple horizontal line).*

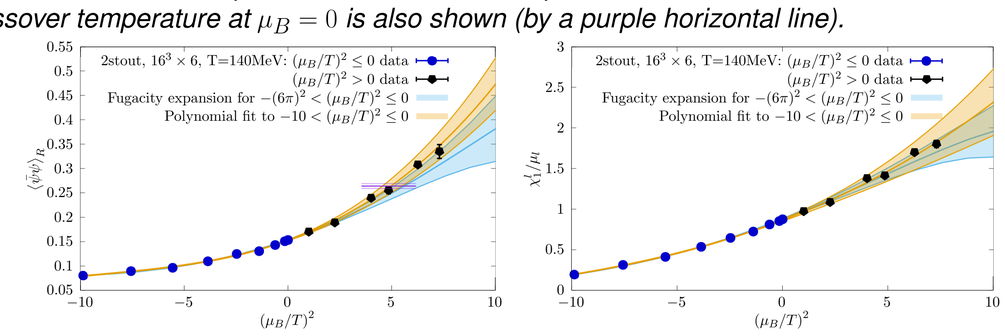

Figure 3: *The renormalized chiral condensate (left) and the light quark number-to-light quark chemical potential ratio (right) as a function of $(\mu_B/T)^2$ at temperature $T = 140$ MeV. Data from simulations at real μ_B (black) are compared with analytic continuation from imaginary μ_B (blue). In the left panel the value of the condensate at the crossover temperature at $\mu_B = 0$ is also shown (purple horizontal line). The simulation data cross this line at $\mu_B/T \approx 2.2$.*

The (bare) light-quark chiral condensate is defined as

$$\langle \bar{\psi}\psi \rangle_{T,\mu} = \frac{1}{Z(T,\mu)} \frac{\partial Z(T,\mu)}{\partial m_{ud}} = \frac{T}{V} \frac{1}{\langle \varepsilon \rangle^{\mathrm{SQ}}_{T,\mu}} \left\langle \varepsilon \frac{\partial}{\partial m_{\mathrm{ud}}} \ln |\mathrm{Re} \det M| \right\rangle^{\mathrm{SQ}}_{T,\mu}. \tag{5}$$

From the bare condensate, the renormalized condensate was obtained with the prescription $\langle \bar{\psi}\psi \rangle_R(T,\mu) = -\frac{m_{ud}}{f_\pi^4} \left[\langle \bar{\psi}\psi \rangle_{T,\mu} - \langle \bar{\psi}\psi \rangle_{0,0} \right]$. We also calculated the light quark density

$$\chi_1^l \equiv \frac{\partial \left(p/T^4\right)}{\partial \left(\mu/T\right)} = \frac{1}{VT^3} \frac{1}{Z(T,\mu)} \frac{\partial Z(T,\mu)}{\partial \hat{\mu}} = \frac{1}{VT^3 \langle \varepsilon \rangle^{\mathrm{SQ}}_{T,\mu}} \left\langle \varepsilon \frac{\partial}{\partial \hat{\mu}} \ln |\mathrm{Re} \det M| \right\rangle^{\mathrm{SQ}}_{T,\mu}. \tag{6}$$

Our results for a temperature scan between 130 MeV and 165 MeV at real chemical potential $\mu_B/T = 1.5, 0$ and $1.5i$ are shown in Fig. 2. We also show that a rescaling of the temperature axis of the form $T \to T \left(1 + \kappa \left(\frac{\mu_B}{T}\right)^2\right)$ collapses the curves into each other. Such a simple rescaling indicates that up to $\mu_B/T = 1.5$ the chiral crossover does not get narrower, which is what one would expect in the vicinity of a critical endpoint. Our results for the chemical potential scan at a fixed temperature of $T = 140$ MeV are shown in Fig. 3. We have performed simulations at $\mu_B/T = 1, 1.5, 2, 2.2, 2.5$. The sign-quenched results are compared with the results of analytic continuation from imaginary chemical potentials. To demonstrate the magnitude of the systematic errors of such an extrapolation we considered two fits. (*i*) As the simplest ansatz, we fitted the data with a cubic polynomial in $\hat{\mu}_B^2 = \left(\frac{\mu_B}{T}\right)^2$ in the range $\hat{\mu}_B^2 \in [-10, 0]$. (*ii*) As an alternative, we also and ansätze for both $\langle \bar{\psi}\psi \rangle_R$ and $\chi_1^l/\hat{\mu}_l$ based on the fugacity expansion $p/T^4 = \sum_n A_n \cosh(n\mu_l/T)$, fitting the data in the entire imaginary-potential range $\hat{\mu}_B^2 \in \left[-(6\pi)^2, 0\right]$ using respectively 7 and 6 fitting parameters. Fit results are also shown in Fig. 3; only statistical errors are displayed. While sign reweighting and analytic continuation give compatible results, in the upper half of the μ_B range the errors from sign reweighting are an order of magnitude smaller. In fact, sign reweighting can penetrate the region $\hat{\mu}_B > 2$ where the extrapolation of many quantities is not yet possible with standard methods [7, 8].

5. Summary

Most lattice studies of hot and dense QCD matter rely on extrapolation from zero or imaginary chemical potentials. The ill-posedness of numerical analytic continuation puts severe limitations on the reliability of such methods. We studied the QCD chiral transition at finite real baryon density with the more direct phase and sign reweighting approaches. We simulated up to a baryochemical potential-temperature ratio of $\mu/T = 2.7$, covering the RHIC Beam Energy Scan range, and penetrating the region where methods based on analytic continuation are unpredictive.This opens up a new window to study QCD matter at finite μ_B from first principles.

6. Acknowledgements

The project was supported by the BMBF Grant No. 05P18PXFCA and by the Hungarian National Research, Development and Innovation Office, NKFIH grant KKP126769. A.P. is supported by the J. Bolyai Research Scholarship of the HAS and by the ÚNKP-21-5 New National Excellence Program of the Ministry for Innovation and Technology. The authors gratefully acknowledge the Gauss Centre for Supercomputing e.V. for funding the project by providing computing time on the GCS Supercomputers JUWELS/Booster and JURECA/Booster.

References

[1] Y. Aoki et al, Nature **443** (2006), 675-678 [arXiv:hep-lat/0611014 [hep-lat]].
[2] C. R. Allton et al, PRD **66** (2002), 074507 [arXiv:hep-lat/0204010 [hep-lat]].
[3] P. de Forcrand et al, NPB **642** (2002), 290-306 [arXiv:hep-lat/0205016 [hep-lat]].
[4] Sz. Borsányi et al, PRD **105** (2022) no.5, L051506 [arXiv:2108.09213 [hep-lat]].
[5] M. Giordano et al, PRD **102** (2020) no.3, 034503 [arXiv:2003.04355 [hep-lat]].
[6] Z. Fodor et al, JHEP **03** (2007), 121 [arXiv:hep-lat/0701022 [hep-lat]].
[7] A. Bazavov et al, PRD **101** (2020) no.7, 074502 [arXiv:2001.08530 [hep-lat]].
[8] Sz. Borsányi et al PRL **125** (2020) no.5, 052001 [arXiv:2002.02821 [hep-lat]].

Presenter: Attila Pásztor (apasztor@bodri.elte.hu)